Field Measurements of Linear and Nonlinear Shear Moduli during Large-Strain Shaking

Benchen Zhang, Farnyuh Menq & Kenneth H. Stokoe II
Civil, Architectural & Environmental Engineering Department, The University of Texas at Austin, Austin, Texas, USA

ABSTRACT: An improvement to the field liquefaction testing method that presently involves one large mobile shaker is under development. The improvement is designed to permit simultaneously determination of both linear and nonlinear shear moduli of soil during large-strain shaking tests. The improved method requires two mobile shakers. Small-amplitude, high-frequency motions (160 Hz) are generated with a small shaker named Thumper. These motions are superimposed on larger-amplitude, lower-frequency motions (25 Hz) generated by a larger shaker named Rattler. By operating the shakers at distinctly different frequencies in perpendicular planes, small-strain shear moduli can be determined at multiple times (>6) during each cycle of higher-strain shaking with Rattler. The Spectral-Analysis-of-Body-Waves (SABW) method is implemented to continuously evaluate the small-strain shear moduli. These initial tests show that the soil skeleton can be studied during larger-strain cycling. The goal is to improve the characterization and understanding of soils undergoing nonlinear loading processes.

1 INTRODUCTION

For the past 14 years, large hydraulic mobile shakers operated by the University of Texas with funding from the National Science Foundation (NSF) have been used to perform nonlinear shaking tests in the field to study the initiation and generation of pore-water pressure leading to soil liquefaction. The current field testing approach involves using one, large mobile shaker to dynamically load the surface of a natural soil deposit with a series of increasing shaking amplitudes. Simultaneously, the motions and pore-water pressure responses are measured at depth in the soil using an embedded array of sensors (Rathje et al. 2005, Cox et al. 2009, Stokoe et al. 2013 and Roberts et al. 2017). The objectives of the field shaking tests are: (1) to measure the excess pore-water pressure generation, and (2) to determine the associated nonlinear shear moduli of the natural sandy deposits as functions of induced cyclic shear strain and number of loading cycles.

During the process of pore-water generation leading to soil liquefaction, the reduction in the shear modulus results from the coupled effects of two processes: (1) the increasing nonlinearity in the soil skeleton as shear strain increases, and (2) the decreasing mean effective confining pressure as pore-water pressure builds up. In an attempt to better understand and characterize this complex behavior, it is important to develop a method with which both linear and nonlinear shear moduli of the soil are determined during large-strain shaking tests. In this initial effort to develop the testing method, a field site with unsaturated soil was selected, and field tests involving numerous low-amplitude to high-amplitude shaking tests were conducted without the added complications of excess pore-water pressure generation.

In this study, two mobile shakers, named Rattler and Thumper, that are available at the NHERI@UTexas equipment facility (Stokoe et al., 2017), were simultaneously used to horizontally load an instrumented soil zone within 1 to 1.5 m of the ground surface. During field testing, Thumper was used to shake the ground surface at 160 Hz with a small force level. At the

same time, Rattler was used to shake the ground surface at 25 Hz over a range of higher force levels. The Spectral-Analysis-of Body-Waves (SABW) method (Kim, 2012) was used to determine the variation of small-strain shear moduli (using the high-frequency, small-strain shear waves induced by Thumper) during the low-frequency, large-strain cyclic loading induced by Rattler. The SABW method and the effects of high-amplitude shearing cycles on the small-strain shear moduli measured at a test site of unsaturated clayey soil in Austin, TX, are presented in this paper.

2 FIELD TEST SITE

Over the past 30 years, many experimental field projects involving soil dynamics and geotechnical earthquake engineering projects have been conducted at the Hornsby Bend Biosolids Management Plant (HBBMP) test site. The test site is owned and operated by the City of Austin. Located southeast of Austin, the HBBMP site is about 3 km north of the Austin-Bergstrom International Airport. Field tests presented in this study were performed in a location named the Lower Tract B at the test site. The ground water table is about 12 m below the ground surface. Disturbed soils samples were recovered using a hand auger within the depth range of the sensor array (1 to 1.5m) for soil classification. The soil in this depth range has a natural water content of 22%, a liquid limit of 29%, and a plasticity index of 10%. The soil is classified as a low-plasticity clay (CL) in the Unified Soil Classification System (USCS). For the purpose of this project, which is to develop a method of simultaneously measuring linear and nonlinear shear moduli, the clayey soil at the site works well, because only one variable, nonlinearity in the soil skeleton as shear strain increases, is affecting the small-strain stiffness of the soil skeleton since the soil is unsaturated.

3 TEST EQUIPMENT

Two, hydraulic mobile shakers and eight, custom-built, 3-D motion sensors were used in these field studies. The shakers and motion sensors are part of the dynamic loading and sensing equipment at the NHERI@UTexas experimental facility (Stokoe et al., 2017). This equipment, which is available as shared-use equipment to any researcher with an NSF-funded project, is discussed below.

3.1 *Hydraulic Mobile Shakers*

Two, hydraulic mobile shakers, named Rattler and Thumper, were used to apply horizontal shaking loads on the ground surface which, in turn, created two sets of vertically propagating shear waves that passed through an embedded array of sensors below the shakers. Photographs of Rattler and Thumper are presented in Figures 1a and 1b, respectively. Rattler is a 22 metric-ton, off-road vehicle upon which a moderate-sized, horizontal shaker is mounted. Rattler is capable of shaking horizontally in the cross-line direction (the direction perpendicular to the longitudinal axis of the mobile shaker) with a maximum shear force of 133 kN over frequencies ranging from 6 and to 80 Hz. Thumper is a 10 metric-ton, International-model 4300 truck to which a

(a) Moderate-capacity shaker named Rattler that is used to create nonlinear soil behavior

(b) Small-capacity shaker named Thumper that is used to continuously evaluate G_{max}

Figure 1. Two hydraulic mobile shakers operated by the NHERI@UTexas equipment facility that were used to evaluate G_{max} continuously during each cycle of large-strain shaking

small-sized shaker is mounted at the rear of the truck. Thumper is capable of shaking horizontally in either the in-line or cross-line directions with a maximum shear force of 26 kN over frequencies ranging from 17 to 300 Hz.

3.2 *Sensor Array*

Eight, custom-built, 3-D motion sensors were used in these studies to create an embedded array of 3-D motion sensors, shown in Figure 2a, which was used to measure ground motions in the X, Y, and Z directions. A photograph of one, 3-D motion sensor is shown in Figure 2b. Each 3-D sensor is composed of: (1) three, 28-Hz geophones (installed orthogonally to measure particle velocities in the X, Y, and Z directions), and (2) a 3-D MEMS accelerometer. The 3-D MEMS accelerometer was used as a tilt sensor in the X and Y directions during sensor installation to measure deviations in the horizontal directions as each 3-D sensor was pushed vertically into the ground. With this information, the final installed locations were determined. The 3-D motion sensors were used to measure ground motions during testing with the shakers. The three geophones and MEMS accelerometer were epoxied in a custom-built, polycarbonate, cone-shape housing.

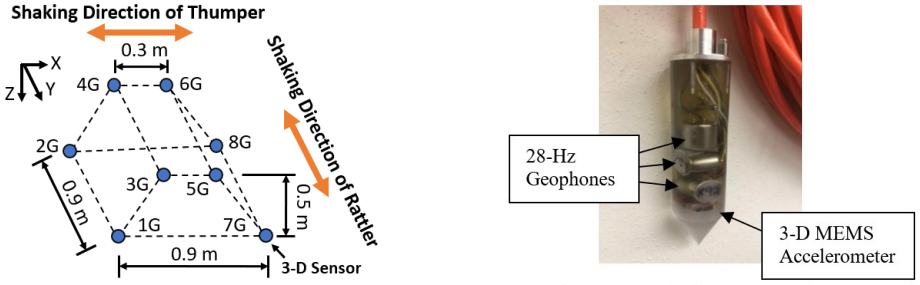

(a) 3-D view of the embedded sensor array (b) Custom-build 3-D motion sensor

Figure 2. Instrumentation used for recording ground motions within the embedded array

As shown in Figure 2a, four of the 3-D motion sensors (3G, 4G, 5G and 6G) were installed at a depth of 1 m, and another four of the 3-D motion sensors (1G, 2G, 7G and 8G) were installed at a depth of 1.5 m. A hydraulic ram mounted at the rear of a third mobile shaker (named T-Rex) was used to push the sensors into the ground. The two sets of four sensors were installed to form two parallel trapezoids in the X-Z plane that were 0.9 m apart laterally. A top view of the sensor array is shown in Figures 3a and a cross-sectional view of one trapezoidal array is shown in Figure 3b.

4 FIELD TESTING PROCEDURE AND EXAMPLE TIME RECORDS

During field testing, Thumper and Rattler were parked next to each other as shown in Figure 4a. The distance between the near edges of the baseplates of Rattler and Thumper was 1 m. Although not presented in this paper, different shaking configurations of the two mobile shakers

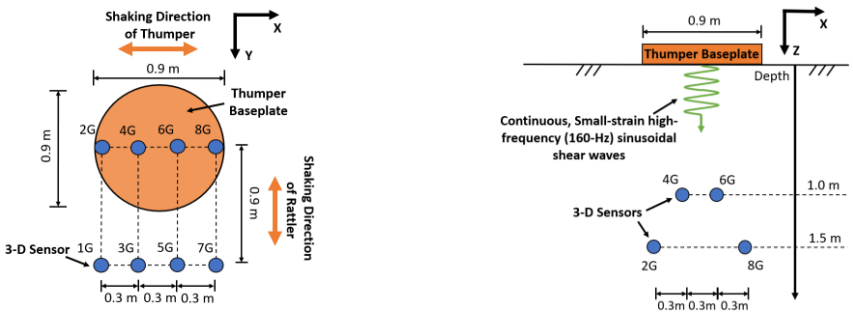

(a) Top view (b) Cross-sectional view

Figure 3. 3-D sensor array installed at the field test site in Austin, Texas

(a) Thumper and Rattler parked side by side

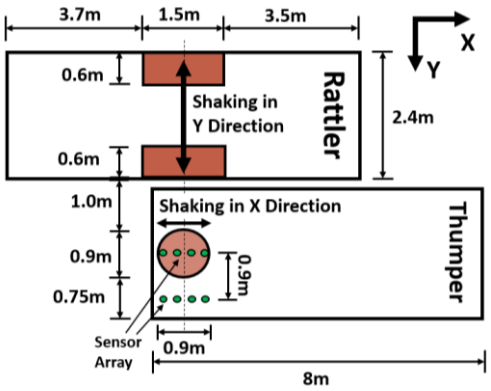

(b) Positions of the trucks in plan view

Figure 4. Positions of the hydraulic shakers during the shaking tests

were also investigated. It was found that by positioning the baseplate of Thumper over one trapezoidal sensor array (2G, 4G, 6G, and 8G) and by locating the baseplate of Rattler as close to the sensor array as possible, the small-amplitude motions generated by Thumper at 160 Hz were clearly and easily recorded during the large-amplitude shaking motions induced by Rattler at 25 Hz (see Figure 4b). The resonant frequency of the field site was found to be 25 Hz. Hence, 25 Hz was chosen to maximize the shear strains generated with Rattler.

Three of the shaking events that were performed at the field site are discussed herein to illustrate the future use of this type of bi-axial loading. The conditions of the shaking events are summarized in Table 1. With both mobile shakers parked as shown in Figure 4, testing began with small-strain uniaxial shaking using only Thumper. This testing condition, presented as Event 1 in Table 1, involved Thumper shaking at a low-force level at 160 Hz so that only small-strain shear moduli in the linear range were determined. Then biaxial loading was performed by shaking with both Thumper and Rattler as presented in Events 2 and 3 in Table 1. Rattler was used to perform an increasing series of staged, higher-force shaking at 25 Hz in the Y direction while Thumper was shaking at 160 Hz in the X direction. This biaxial shaking condition allowed evaluation of the effects of larger shear strains in the Y direction on the small-strain shear modulus (G_{max}) in the X direction. In Events 2 and 3, the shakers were loading in perpendicular directions because it was found, as expected, that the signals are easier to process when the polarization of shear waves at two independent frequencies are in perpendicular planes. It is planned to investigate the effect of larger cyclic loading on the small-strain G_{max} values in the same plane in future testing by having the two shakers load in the same direction.

Example time-displacement records collected with sensor 6G in the X and Y directions during Events 1 and 2 are shown in Figure 5. The displacement-time histories are integrated from the velocity-time histories measured by the X and Y geophones in sensor 6G. The time records in both the X and Y directions contain 5 tapered cycles at the beginning and end of each shaking event. The tapered cycles are applied to protect the hydraulic shakers from abrupt starting and stopping. In shaking Event 1 (Figures 5a and 5c), sensor 6G monitored the 160-Hz sinusoidal signal in the X direction and showed essentially no signal in the Y direction; hence, essentially no cross-coupling in the 3-D sensor at this shaking level. The 160-Hz sinusoidal signal was used to calculate the small-strain shear moduli using the SABW method as discussed in Section 6. In shaking Event 2 (Figures 5b and 5d), sensor 6G monitored the 160-Hz sinusoidal signal in the X direction (generated by Thumper) and the 25-Hz sinusoidal signal in the Y direction (generated

Table 1. Shaking configurations and induced shear strains in three, shaking events

Event No.	Low level shaking with Thumper			High level shaking with Rattler		
	Shaking Direction	Frequency Hz	Shear strain %	Shaking Direction	Frequency Hz	Shear strain %
1	X	160	0.001	-	-	-
2	X	160	0.001	Y	25	0.01
3	X	160	0.001	Y	25	0.03

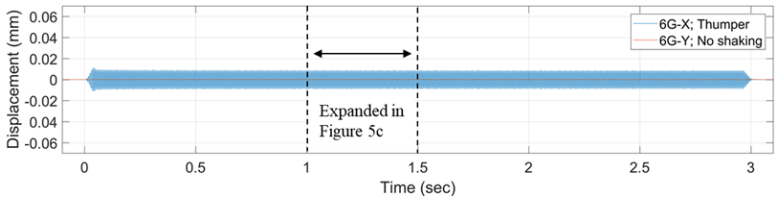

(a) Event 1: Only Thumper shaking at 160 Hz in the X direction

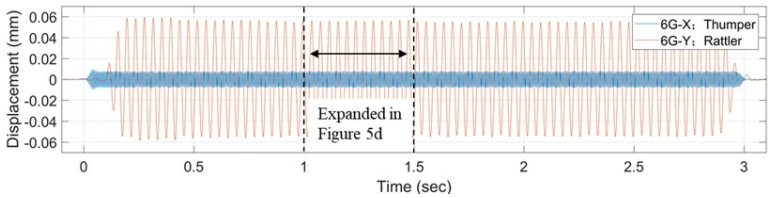

(b) Event 2: Thumper shaking at 160 Hz in the X direction while Rattler is shaking at 25 Hz in the Y direction

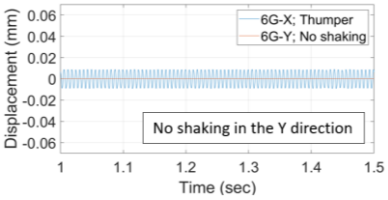

(c) Expanded area in Figure 5a

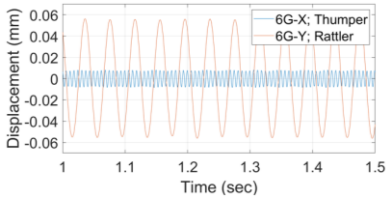

(d) Expanded area in Figure 5b

Figure 5. Time records of motion from sensor 6G in the X and Y directions when only Thumper was shaking (Event 1) and when both Thumper and Raptor were shaking (Event 2)

by Rattler). During the steady-state shaking between the tapered starting and ending cycles, the displacement amplitude of the 25-Hz shear-wave signal in the Y direction was about 7 times larger than the 160-Hz shear-wave signal in the X direction.

5 SHEAR STRAIN EVALUATIONS

Cyclic shear strains in the instrumented soil zone were calculated using the 3-D sensor array shown in Figure 3. Two different approaches were used in this study to evaluate shear strain induced by the two mobile shakers. Rathje et al. (2005) categorized these two approaches as: (1) the displacement-based (DB) method, and (2) the wave propagation-based (WPB) method. The WPB method was used to analyze the 160-Hz, small-strain shaking by Thumper and the DB method was used to analyze the 25-Hz, larger strain shaking created with Rattler as discussed below.

The wave propagation-based (WPB) method utilizes the ratio of particle velocity to wave-propagation velocity to compute shear strain. The assumption made in this strain computational procedure is that one-dimensional (1-D) stress wave propagation is occurring (also termed plane-wave propagation). The in-plane shear strain, γ, induced in the sensor array is simply:

$$\gamma = \frac{-\dot{u}}{V_{s,vh}} \tag{1}$$

where $\dot{u}$ is the horizontal, in-line particle velocity, and $V_{s,vh}$ is the shear wave velocity of a vertically propagating, horizontally polarized shear wave. The minus sign in Equation 1 indicates that strain is 180 degrees out of phase with particle velocity.

The displacement-based (DB) method uses displacement-time histories measured with four motion sensors to evaluate shear-strain time histories. In this study, the four motion sensors were chosen to create an inclined rectangular array so that a 4-node iso-parametric element formulation could be applied to the plane in which the four sensors were located. For example, when Rattler is shaking in the Y direction in Event 2 and 3, four sensors (5G, 6G, 7G and 8G) are used as the four nodes of the inclined rectangular array to evaluate the shear strain of soil between sensors 6G and 8G in YZ plane.

Studies by Cox et al., 2009 show that larger shear strains should be evaluated by the DB method because this method accounts for the vertical displacements in the motions created by the larger rocking motions of the baseplate that occur during horizontal shaking. The DB method was, therefore, used to calculate shear strains induced by Rattler shaking with high-force levels at 25 Hz. Although the DB method is more reliable at larger shear strains, the DB method is not suitable for high-frequency (short-wavelength) measurements. When the wavelength is less than 5 times the sensor spacing, the assumption of linear variable displacement used in the DB method is not valid (Rathje et al. 2005). In shaking Event 1, the SABW analysis (discussed in Section 6) shows that the average velocity of the sinusoidal, 160-Hz shear wave is 96 m/s. This shear wave has a wavelength of 0.6 m, which is only 1.2 times the vertical spacing between geophone pairs (0.5 m). As a result, the WPB method is used to calculate the shear strain induced by the low-amplitude shaking of Thumper at this frequency.

6 SPECTRAL-ANALYSIS-OF-BODY-WAVES (SABW) METHOD

The Spectral-Analysis-of-Body-Waves (SABW) method (Kim, 2012) was implemented to permit determination of small-strain shear moduli continuously during the higher-strain loading cycles. The method is briefly outlined due to space limitations. Implementation of the method can be divided into two steps. The first step involves determining the phase shift in the frequency domain between the sinusoidal signals from the two receivers at different depths. Using the Fast Fourier Transform (FFT) algorithm, the time-domain records ($x(t)$ and $y(t)$) collected from two sensors are transformed into the frequency-domain ($X(f)$ and $Y(f)$). The transfer function, $H_{YX}(f)$, is determined as the ratio of $Y(f)$ over $X(f)$. The phase component, $\phi(f)$, of $H_{YX}(f)$ is calculated and indicates the phase shift between the time-domain records $x(t)$ and $y(t)$. In the second step, the unwrapped phase shift, ϕ, and the distance, d, that the shear wave traveled are used to calculate the wavelength of the shear wave ($\lambda = d \times (2\pi/\phi)$). Shear wave velocity, V_s, is simply calculated using the excitation frequency, f, and wavelength ($V_s = f \times \lambda$). Small-strain shear modulus, G_{max}, is simply calculated using the total unit weight, γ_t, gravitational acceleration, g, and V_s ($G_{max} = (\gamma_t/g) \times {V_s}^2$).

The analysis of two time-domain signals recorded by the 6G and 8G sensor pair in shaking Event 1 is shown in Figure 6 to illustrate how the value of G_{max} is calculated cycle by cycle using the SABW method. Particle velocity signals recorded by motion sensors 6G and 8G (depths of 1.0 and 1.5 m, respectively) in the X direction from 1.00 to 1.20 seconds are plotted in Figure 6a. Both signals contain 30 cycles of 160-Hz sinusoids, with the first six cycles designated by numbers 1 through 6. In Figure 6b, the truncated signals of the 6th cycle from both sensors are shown. The SABW procedure as described above is used to calculate the shear wave velocity and then the shear modulus for the sixth cycle. The phase difference of the truncated signals was determined to be 5.3 radius. The vertical distance between sensors 6G and 8G in the array is 0.50 m (Figure 3). The wavelength is calculated to equal 0.60 m which results in a shear wave velocity equal to 96 m/s. The total unit weight of the soil is estimated to be 18.5 kN/m^3 so that a shear modulus of 17 MPa is calculated.

This SABW procedure is used to calculate shear wave velocities and shear moduli during every small-strain cycle at 160 Hz. The resulting shear wave velocities over cycles from 1.00 to 1.20 seconds are presented in Figure 6c. Each shear wave velocity value is plotted at the time in the middle of the two sinusoidal cycles. It can be seen in Figure 6c that the shear wave velocities are constant over these 30 cycles of small-strain uniaxial loading just as expected.

7 TEST RESULTS

The peak shear strains induced by Thumper and Rattler in the soil between sensors 6G and 8G during the three shaking events discussed in Section 4 are presented in Table 1. In uni-axial shaking Event 1, Thumper induced a peak shear strain of 0.001% in the instrumented soil zone in the XZ plane. The soil exhibited linear-elastic behavior at this small strain level. In bi-axial shaking Events 2 and 3, Rattler generated shear strains of 0.01% and 0.03% in the YZ plane. In this case, the low-plasticity clay exhibited only mild nonlinear behavior in the YZ plane which

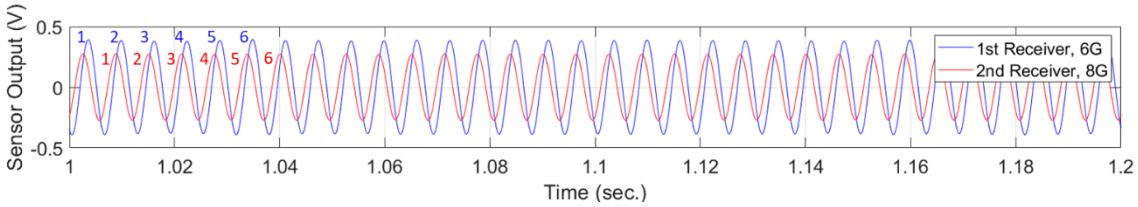

(a) Time records of 6G and 8G in shaking Event 1; excitation frequency = 160 Hz

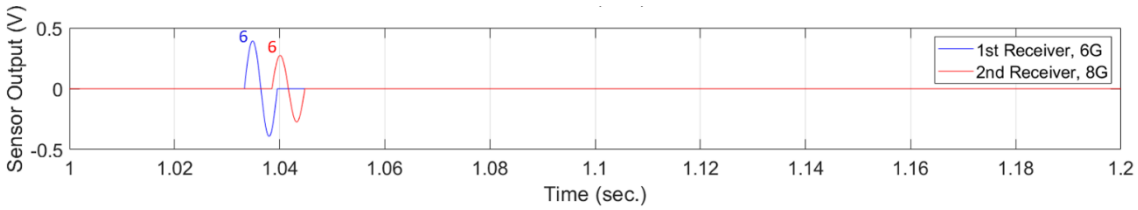

(b) Truncated signals representing the 6th cycle of the original signals in Figure 6a

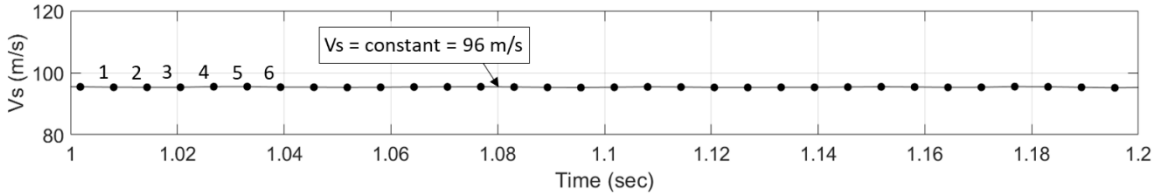

(c) Shear wave velocities calculated cycle by cycle for the original signals in Figure 6a

Figure 6. The SABW method used to evaluate the cycle-by-cycle, small-strain, shear wave velocities

was independent of number of loading cycles; hence, exhibited no degradation. On the other hand, the values of G_{max} in the XZ plane determined with the 160-Hz shaking did vary systematically as discussed below.

A hysteresis loop representing one cycle of the stress-strain relationship during the 25-Hz loading in the YZ plane in shaking Events 2 and 3 is schematically shown in Figure 7. The hysteresis loop is similar for shaking Events 2 and 3, only the slope and area change. (The values of G in the YZ plane were constant and equaled 16.4 MPa and 13.6 MPa in Events 2 and 3, respectively). The small-strain shear modulus (G_{max}) values in the XZ plane are denoted as G1 through G7 in Figure 7. The G_{max} values were determined, on average, 6.4 times during each cycle of the 25-Hz stress-strain loops in the YZ plane. These G_{max} values calculated from 1.0 to 1.5 seconds in the three shaking events are shown in Figure 8. In shaking Event 1 (Figure 8a), the small-strain shear moduli are constant over all loading cycles. In shaking Events 2 and 3 (Figures 8b, and 8c, respectively), it can be seen that the values of G_{max} fluctuate sinusoidally at a frequency of 25 Hz, the frequency of the larger-amplitude shaking.

The systematic oscillation of G_{max} in the XZ plane in Events 2 and 3, the decrease in the average value of G_{max} in the XZ plane as the shear strain increases in the YZ plane, and the lack of any changes during Event 2 and 3 with number of cycles in degradation combine to indicate the potential of this field method to help characterize the soil skeleton during nonlinear loading processes. However, more field investigations are required, and this research is continuing. For instance, one would expect the G_{max} values in the XZ plane at both ends of the stress-strain loop shown in Figure 7 to be equal if the shear strain in the ground is zero; hence, G_{max} will peak

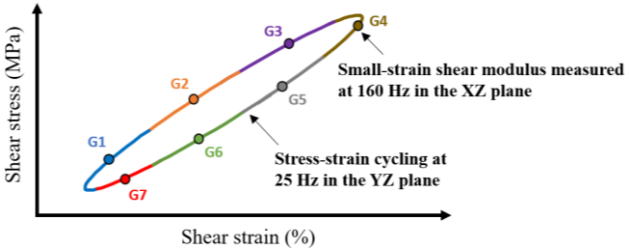

Figure 7. Schematic representation of small-strain shear moduli in the XZ plane during one, high-amplitude loading cycle generated by Rattler in the YZ plane

twice in each hysteresis loop of the larger-amplitude shaking and the oscillation of G_{max} will be at 50 Hz. However, if the initial shear strain is greater than zero and the unloading side of the hysteresis loop does not reach the side of negative shear strain, there will be only one peak value of G_{max} in each hysteresis loop. The 25-Hz oscillations shown in Figures 8b and 8c, indicate the initial shear strain is greater than zero and the unloading side of the hysteresis loop does not cross the zero shear strain line. Similar results were observed in laboratory using a cyclic triaxial device with bending elements (Ueno et al., 2019).

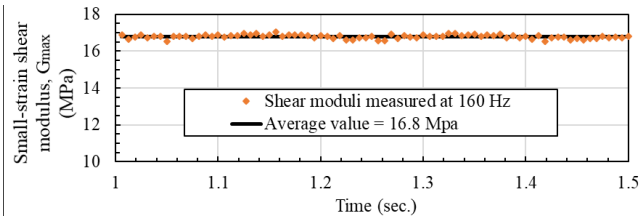

(a) Event 1: Only Thumper shaking in the X direction; peak shear strain in the XZ plane equals 0.001%

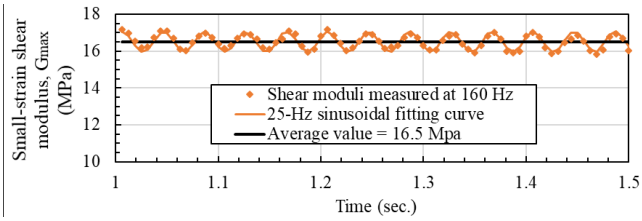

(b) Event 2: Thumper and Rattler shaking simultaneously; peak shear strain in the YZ plane equals 0.01%

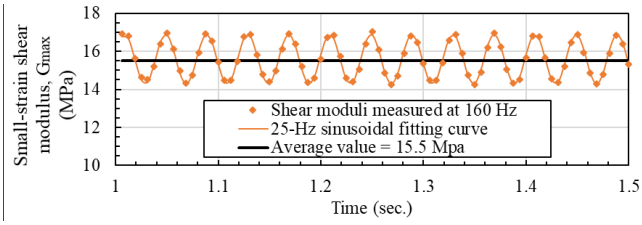

(c) Event 3: Thumper and Rattler shaking simultaneously; peak shear strain in the YZ plane equals 0.03%

Figure 8. Small-strain shear moduli evaluated by the SABW methods at 160 Hz in the XZ plane

8 CONCLUSIONS

During field shaking tests to determine soil liquefaction, the shear modulus of the sandy soil decreases as a result of both nonlinearity in the soil skeleton and decreasing effective stress due to increasing pore-water pressure. To better understand the impact of these two processes, an improvement to the field testing method that involves two hydraulic mobile shakers is being developed. The goal is to measure the variation of small-strain shear moduli of soil skeleton during cycles of higher-amplitude shaking. The small-strain shear moduli are measured in a plane perpendicular to that of the larger-strain shaking. In these initial tests which only involved unsaturated clayey soil, the improved field method was shown to be capable of measuring the reduction in the small-strain shear moduli of the soil skeleton due to the effect of higher-amplitude shaking. The reduction in the small-strain shear modulus of the soil skeleton due to pore-water pressure generation will be studied in future work.

9 ACKNOWLEDGEMENTS

The authors would like to thank the U.S. National Science Foundation (NSF) for the financial support to develop and operate the NHERI@UTexas Equipment under grants CMS-0086605, CMS-0402490, and CMMI-1520808 and the financial support for this research project under grant CMMI-1663654. Special thanks also go to the staff at the University of Texas at Austin including Mr. Andrew Valentine and Mr. Robert Kent who assisted in the field work.

10 REFERENCES

Cox, B. R., Stokoe, K. H., & Rathje, E. M. 2009. An In Situ Test Method for Evaluating the Coupled Pore Pressure Generation and Nonlinear Shear Modulus Behavior of Liquefiable Soils. Geotechnical Testing Journal 32(1): 11-21.

Kim, C. Y. 2012, Development of the Spectral-Analysis-of-Body-Waves (SABW) Method for Downhole Seismic Testing with Boreholes or Penetrometers. Ph.D. Dissertation, The University of Texas at Austin, Austin, Texas.

Rathje, E.M., Chang, W.J. & Stokoe, K.H. 2005. Development of an In Situ Dynamic Liquefaction Test. ASTM Geotechnical Testing Journal 28(1): 50-60.

Roberts, J.N., Stokoe, K.H., Cox, B., & Menq, F. 2017. Field and Laboratory Investigations into the Behaviors of Silty Sands that Leads to Liquefaction Triggering. 16th World Conference on Earth-quake. Santiago: Chile.

Stokoe, KH, Roberts, JN, Hwang, S, Cox, B, Menq, FY & Van Ballegooy, S. 2014. Effectiveness of inhibiting liquefaction triggering by shallow ground improvement methods: Initial field shaking trials with T-Rex at one site in Christchurch, New Zealand. New Zealand - Japan Workshop on Soil Liquefaction during Recent Large-Scale Earthquakes, Auckland, pp. 193-202.

Stokoe, K.H., Cox, B., Clayton, P. & Menq, F. 2017. NHERI@UTEXAS experimental facility: large-scale mobile shakers for natural-hazards field studies, 16th World Conference on Earthquake. Santiago: Chile

Ueno, K., Kuroda, S. Hori, T. & Tatsuoka, F. 2019. Elastic shear modulus variations during un-drained cyclic loading and subsequent reconsolidation of saturated sandy soil. Soil Dynamics and Earthquake Engineering 116(2019): 476-489.